Journal of Physical and Theoretical Chemistry
of Islamic Azad University of Iran, 14 (1) 63-80: Spring 2017
(J. Phys. Theor. Chem. IAU Iran)
ISSN 1735-2126

Interaction of SO_2 gas with the pristine and B&O atoms doped AlNNTs: A DFT study

Mahdi Rezaei−Sameti* and Mahdieh Bagheri
Department of Applied Chemistry, Faculty of Science, Malayer University, Malayer, 65174, Iran

Received July 2017; Accepted August 2017

ABSTRACT

In this research, the effects of B, O and B&O−doped on the SO_2 gas adsorption on the surface of the (4, 4) armchair AlNNTs are investigated by using DFT method. From optimized structures the geometrical and electrical properties, adsorption energy, gap energy, global hardness, electrical potential, HOMO−LUMO orbitals, density of states (DOS) plots, electrostatic potential (ESP) plots and NMR parameters are calculated and are analyzed. The adsorption energy of the all adsorption models is negative and exothermic in thermodynamic view of point. Doping of B atom increases the adsorption energy of nanotube/SO_2 complex, whereas doping O atom decreases the adsorption energy of system. The positive values of ΔN of nanotube/SO_2 complex indicate that the charge transfer occur toward to the SO_2 gas, which suggests that their electronic properties of system could be notably changed upon chemisorption's of SO_2. The NMR results reveal that the isotropy the electrostatic properties of nuclei are mainly dependent on electronic density at their sites, therefore because of the SO_2 gas adsorption, the electronic densities of nuclei and the CS tensors undergo changes.

Keywords: AlNNTs; (B, O and B&O−doped); SO_2 adsorption; DFT; MEP; NMR

INTRODUCTION

After discovery of carbon nanotubes (CNTs) and other nanotubes the extensive research activity within the past decade have been developed to study the structural, electrical, syntheses and application of nanoscale materials in nano engineering and electronic products [1−6]. The aluminum nitride nanotubes (AlNNTs) is attracted the attention of many researchers, due to the largest band gap, semiconductor properties, high thermal conductivity, and mechanical strength. The AlNNTs is extensively used to the high electrical resistivity, reliable dielectric properties, technological applications, resistance toward chemicals and gases, mainly in micro and optoelectronics such as laser diodes and solar−blind ultraviolet photo detectors and semiconductors [7−10]. These properties make AlNNTs ideal as a substrate material for electronic devices, particularly power integrated circuits and it adaptable to a large variety of environments and enables large freedom in its device fabrication, such as in electrical packaging and in composites [11−14].

In recent years the development of industrial products and environmental pollutions are caused that many researches have been focused on development of suitable gas sensitive materials for

*Corresponding author: mrsameti@gmail.com, mrsameti@malayeru.ac.ir

continuous monitoring and setting off alarms for hazardous chemical vapors beyond the specified level. For these aims, the extensive studies are done to the structural, electrical properties and applications of AlNNTs for detecting and adsorbing different toxic and pollution material [15−51].

Sulfur dioxide (SO_2) is one of the major gaseous pollutants and has significant impacts upon human health. The concentration of sulfur dioxide in the atmosphere can influence the habitat suitability for plant communities, as well as animal life. Sulfur dioxide emissions are a precursor to acid rain and atmospheric particulates [52−53]. In the recent years, many detectors, sensors absorber have been developed to monitor and adsorb SO_2 gas with acceptable level of accuracy [54−58].

In this research we consider 22 different configuration models for adsorbing SO_2 gas on the surface of the pristine and B&O atoms doped of (4, 4) armchair AlNNTs. The structural properties, chemical reactivity, the difference between the HOMO and LUMO orbitals for the energy gap, the adsorption energy, and the molecular electrostatic potentials are calculated to investigate the electronic structures of nanotube/SO_2 complex. The results of this research may be useful for making a sensor or adsorbent for SO_2 gas.

COMPUTATIONAL METHODS

In this study, at the first step, we consider several different orientations and configurations for adsorbing SO_2 gas on the surface of the pristine, B, O, and B&O doped AlNNTs. After optimizing all considered configurations, we select 22 configurations for (4, 4) armchair models of AlNNTs, in which the open ends of nanotube are terminated by 16 hydrogen atoms in order to avoid dangling bonds and decrease calculation time.

Here the A, B, C, D and E models are utilized for exhibiting the adsorption SO_2 gas on the surface of the Al and N atoms of pristine, O, B and B&O doped of (4, 4) armchair AlNNTs respectively. The a, b and c indexes are used for denoting the adsorption of SO_2 gas from S site, parallel sites and O sites on the outer surface of nanotube respectively. The d and e indexes are used for denoting the SO_2 adsorption from backward of doping layer and inner layers of nanotube respectively (see Fig.1). All selected models are individually optimized by using DFT method at cam−B3LYP level of theory using the 6−31G (d) base set [59] with performing the GAMESS suite of programs [60−61]. From optimized results, the adsorption energy (E_{ads}) of SO_2 gas on the surface of nanotube is calculated as follows:

$$E_{ads} = E_{AlNNTs/SO_2} - (E_{AlNNTs} + E_{SO_2}) + BSSE \quad (1)$$

Here E_{AlNNTs/SO_2}, E_{AlNNTs} and E_{SO_2} obtained from the scan of the potential energy of the AlNNTs/SO_2 complex, AlNNTs and SO_2 respectively and the BSSE is base set superposition error.

From the highest occupied molecular orbital (HOMO) and the lowest unoccupied molecular orbital (LUMO) the gap energy (E_{gap}), electronic chemical potential (μ), global hardness (η), electronegativity of nanotube (χ), electrophilicity index (ω), global softness (S) and charge transfer parameters (ΔN) of the of these compounds are calculated by Eqs (2−9) [62−63].

$$Egap = E_{LUMO} - E_{HOMO} \quad (2)$$

$$\mu = -(I + A)/2 \quad (3)$$

$$\eta = (I - A)/2 \quad (4)$$

$$\chi = -\mu \quad (5)$$

$$\omega = \mu^2 / 2\eta \quad (6)$$

$$S = 1/2\eta \quad (7)$$

$$E_{FL} = (E_{HOMO} + E_{LUMO})/2 \quad (8)$$

$$\Delta N = (-\mu/\eta) \quad (9)$$

Where I (E_{HOMO}) is the ionization potential and A (E_{LUMO}) the electron affinity of the molecule.

RESULTS AND DISCUSSION

Structural and geometrical parameters

The 22 optimized adsorption models (A−a to E−e models) are shown in Fig.1. From the optimized structures, the geometrical parameters involve the bond length and bond angle are calculated. Based on the obtained results, in the pristine AlNNTs, the average Al–N bond length is equal 1.81 Å. According to our theoretical results, in all of optimized models, when the SO_2 gas adsorb on the surface of the nanotube, three Al–N bond lengths of the surrounding of the adsorbing position slightly change compare to these bond lengths in the pristine nanotube. This result indicates weakening of the bonds around the interaction site, due to the interaction between SO_2 gas and the AlNNTs.

With doping B and O atoms the bond length decrease significantly from original values due to different radius of doping atoms with respect to Al and N atoms of nanotube. The bond length and bond angle of nanotube alter slightly from original values due to SO_2 adsorption on the exterior and interior surface of nanotube.

The calculated adsorption energy (E_{ads}) for all models are given in Tables (1–3). Inspections of results reveal that the adsorption energy of all adsorption models is negative and all adsorption models are exothermic and favorable in thermodynamic view of point. The

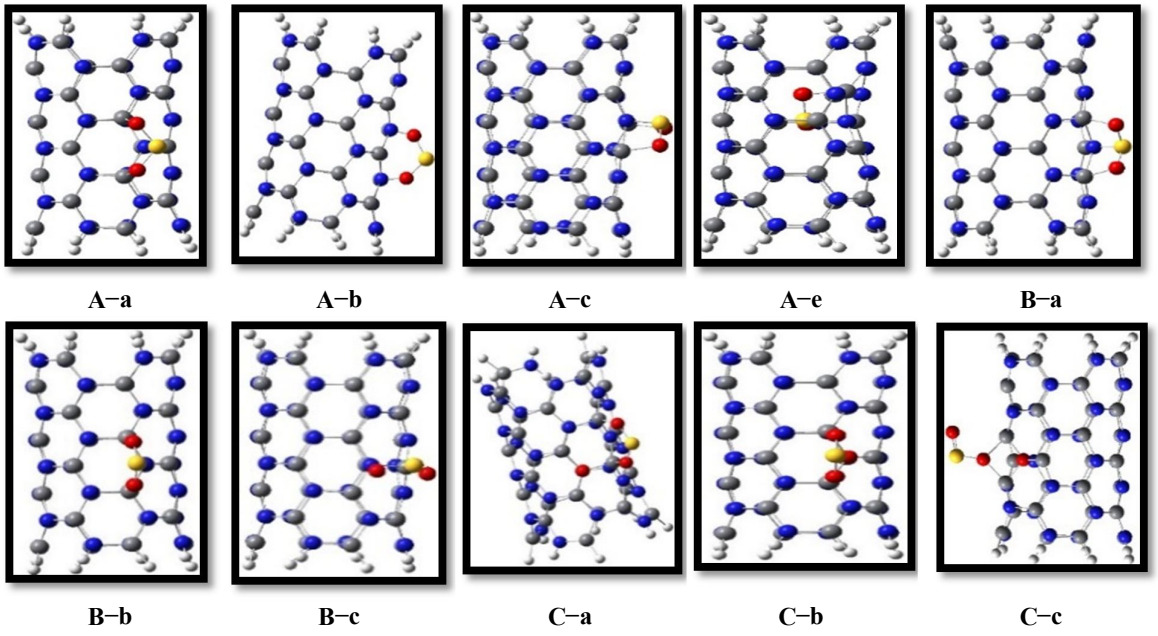

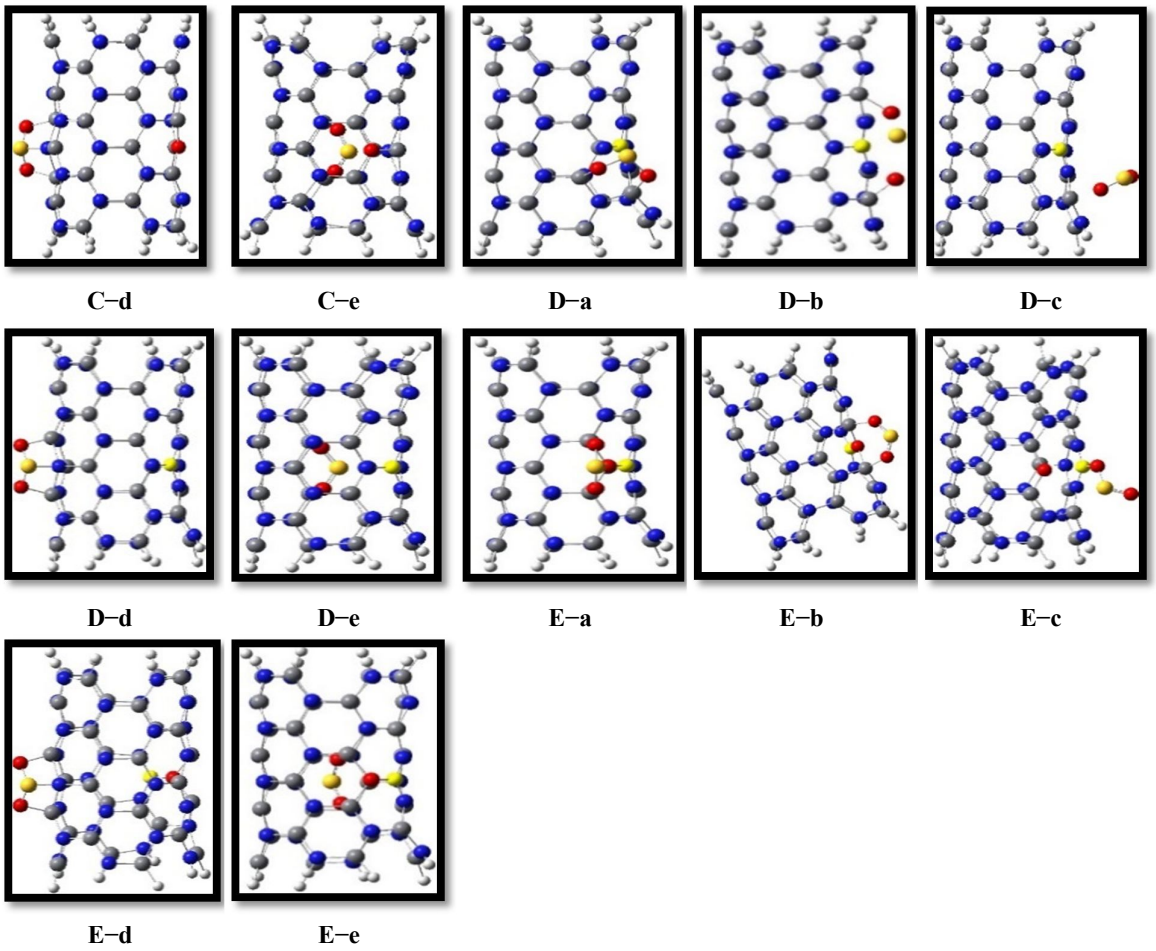

Fig. 1. 2D views of SO_2 gas adsorption on the surface of pristine and B, O and B&O doped of (4, 4) armchair model of AlNNTs for (A−a to E−e models).

adsorption energy of the all models is in range −3.76 to −106.7Kcal/mol. Comparing results show that the adsorption energy of C−b model is −106.7Kcal/mol and is more than other those models, and the D−e model with −3.76 Kcal/mol has lower than other those models. Doping of B atom at the C models increase the adsorption energy of system significantly from original values, whereas doping O atom in D models decrease it from original values.

The adsorption energies of (a) index of all models are in order: C−a>E−a>A−a=B−a>D−a.

On the other hand the adsorption energy of SO_2 gas in the inner layer of nanotube is in order:

E−e> C−e> A−e=B−e> D−e. The BSSE values all adsorption models are in range 0.0002 to 0.0035. The adsorption energy results suggest that the interaction in all adsorption models belong to chemisorption. It can be concluded that SO_2 experiences a chemisorption interaction with the pristine and B, O and B&O−doped AlNNTs surface, with a significant change in its structure with respect to the gas−phase molecule.

Table 1 Quantum parameters of SO_2 adsorption on the surface of pristine and O− doped AlNNTs Models A, B and D

	A−a	A−b	A−c	A−e B−e	B−a	B−b	B−c	D−a	D−b	D−c	D−d	D−e
Ead / Kcal/mol	−50.84	−14.95	−44.38	−7.91	−50.84	−14.95	−8.84	−38.44	−76.21	−11.27	−51.44	−3.74
E(HOMO)/ev	−6.17	−6.28	−6.38	−6.35	−6.41	−6.08	−5.8	−5.77	−5.78	−6.08	−6.37	−6.35
E (LUMO)/ ev	−2.60	−2.97	−1.98	−2.05	−2.00	−5.20	−2.1	−2.41	−2.22	−4.91	−1.92	−3.32
E(gap)/ev	3.57	3.31	4.40	4.29	4.41	0.88	3.73	3.35	3.56	1.17	4.45	3.03
E $_{FL}$/ ev	−4.39	−4.62	−4.18	−4.20	−4.21	−5.64	−3.9	−4.09	−4.00	−5.49	−4.14	−4.83
I/ ev	6.17	6.28	6.38	6.35	6.41	6.08	5.82	5.77	5.78	6.08	6.37	6.35
A/ ev	2.60	2.97	1.98	2.05	2.00	5.20	2.09	2.41	2.22	4.91	1.92	3.32
μ/ ev	−4.39	−4.62	−4.18	−4.2	−4.21	−5.64	−3.9	−4.09	−4.00	−5.49	−4.14	−4.83
χ/ ev	4.39	4.62	4.18	4.2	4.21	5.64	3.95	4.09	4.00	5.49	4.14	4.83
η/ ev	1.78	1.65	2.20	2.15	2.20	0.44	1.86	1.68	1.78	0.58	2.22	1.51
S/(ev)$^{-1}$	0.89	0.83	1.10	1.07	1.10	0.22	0.93	0.84	0.89	0.29	1.11	0.76
ω/ ev	5.40	6.45	3.97	4.10	4.02	3.61	4.19	4.99	4.50	4.98	3.86	7.72
Δφ/ev	4.39	4.62	4.18	4.20	4.21	5.64	3.95	4.09	4.00	5.49	4.14	4.83
ΔN/ev	2.46	2.79	1.90	1.95	1.91	12.82	2.12	2.44	2.25	9.46	−1.86	3.20

Table 2 Quantum parameters of SO_2 adsorption on the surface of pristine and B− doped AlNNTs Models C. (1 and 2 represent the α and β spin)

	C-a-α	C-a-β	C-b-α	C-b-β	C-c-α	C-c-β	C-d-α	C-d-β
Ead / Kcal/mol	-104.99		-106.70		-81.73		-51.82	
E(HOMO)/ev	−5.88	−5.91	−6.29	−6.30	−6.39	−6.26	−3.76	−6.32
E (LUMO)/ ev	−4.19	−1.93	−3.65	−1.95	−3.08	−1.99	−1.91	−2.21
E(gap)/ev	1.69	3.98	2.64	4.35	3.31	4.27	1.85	4.11
E $_{FL}$/ ev	−5.03	−3.92	−4.97	−4.12	−4.73	−4.12	−2.83	−4.26
I/ ev	5.88	5.91	6.29	6.30	6.39	6.26	3.76	6.32
A/ ev	4.19	1.93	3.65	1.95	3.08	1.99	1.91	2.21
μ/ ev	−5.03	−3.92	−4.97	−4.12	−4.73	−4.12	−2.83	−4.26
χ/ ev	5.03	3.92	4.97	4.12	4.73	4.12	2.83	4.26
η/ ev	0.85	1.99	1.32	2.17	1.65	2.13	0.92	2.05
S/(ev)$^{-1}$	0.42	0.99	0.66	1.09	0.83	1.07	0.46	1.03
ω/ ev	4.93	3.85	4.69	3.91	6.78	3.98	4.35	4.43
Δφ/ev	5.03	3.92	4.97	4.12	4.73	4.12	2.83	4.26
ΔN/ev	5.94	1.97	3.76	1.90	2.87	1.93	3.08	−2.08

Table 3 Quantum parameters of SO_2 adsorption on the surface of pristine and B&O doped AlNNTs Models E. (1 and 2 represent the α and β spin)

	E−a−α	E−a−β	E−b−α	E−b−β	E−c−α	E−c−β	E−d−α	E−d−β	E−e−α	E−e−β
Ead / Kcal/mol	−99.05		−99.05		−53.81		−52.11		−65.47	
E(HOMO)/ev	−6.02	−6.05	−6.02	−6.05	−6.54	−6.46	−4.43	−6.46	−6.36	−6.27
E (LUMO)/ ev	−4.35	−1.75	−4.35	−1.75	−3.52	−2.02	−1.85	−2.28	−3.90	−1.72
E(gap)/ev	1.66	4.30	1.66	4.30	3.02	4.44	2.58	4.18	2.46	4.55
E $_{FL}$/ ev	−5.18	−3.90	−5.18	−3.90	−5.03	−4.24	−3.14	−4.37	−5.13	−3.99
I/ ev	6.02	6.05	6.02	6.05	6.54	6.46	4.43	6.46	6.36	6.27
A/ ev	4.35	1.75	4.35	1.75	3.52	2.02	1.85	2.28	3.90	1.72
μ/ ev	−5.18	−3.90	−5.18	−3.90	−5.03	−4.24	−3.14	−4.37	−5.13	−3.99
χ/ ev	5.18	3.90	5.18	3.90	5.03	4.24	3.14	4.37	5.13	3.99
η/ ev	0.83	2.15	0.83	2.15	1.51	2.31	1.29	2.09	1.23	2.27
S/(ev)$^{-1}$	0.41	1.07	0.42	1.07	0.75	1.15	0.64	1.04	0.61	1.14
ω/ ev	16.17	3.54	16.19	3.54	8.38	3.89	3.82	4.57	10.70	3.51
Δφ/ev	5.18	3.90	5.18	3.90	5.03	4.24	3.14	4.37	5.13	3.99
ΔN/ev	6.24	1.81	6.24	1.81	3.33	3.89	−2.43	2.09	4.17	1.76

By using the adsorption energy, the recovery time of the sensor device based on the conventional transition state theory is calculated by Eq. 10.

$$\tau = \nu_0^{-1} \exp^{(-Ead/kT)} \quad (10)$$

where T is temperature, k is the Boltzmann's constant, and ν_0 is the attempt frequency. According to this equation, the increase in the adsorption energy leads to an increment in the recovery time and the stronger interactions between nanotube and adsorbate. Inspection of results in Tables (1−3), it can find that the more negative values of adsorption energies for the C−a, C−b, C−c, E−a and E−b models are caused that the recovery time of these models are more than other those models. Thereby the interaction of SO_2 gas with the B and B&O‐doped AlNNTs is stronger than other models. While the less negative values of adsorption energy for D−e, A−e, B−c, D−c, A−b and B−b models indicate that the recovery time for these models are lower than those other models and so the interaction and adsorption of SO_2 molecule in this forms are weaker than those other models.

The recovery time result demonstrate that the B and B&O‐doped AlNNTs models are a good candidate to making the absorber for SO_2 gas and the pristine and O‐doped AlNNTs are a good candidate for making the sensor and detecting of SO_2 gas.

HOMO and LUMO Orbital analysis

To obtain a better understanding about the interaction between SO_2 gas and the pristine, B, O, and B&O‐doped AlNNTs, the highest occupied molecular orbital (HOMO) and lowest unoccupied molecular orbital (LUMO) are calculated and the all HOMO−LUMO plots are displayed in Fig 2. As can be seen in Fig. 2, the HOMO orbitals of the all adsorption models are localized on the surface nanotube around adsorbing position except the C−d, C−e, D−a, D−d, E−d and E−e models. The HOMO orbital densities of the C−d, C−e, E−d and E−e adsorption models are localized on the forward layer of adsorption position.

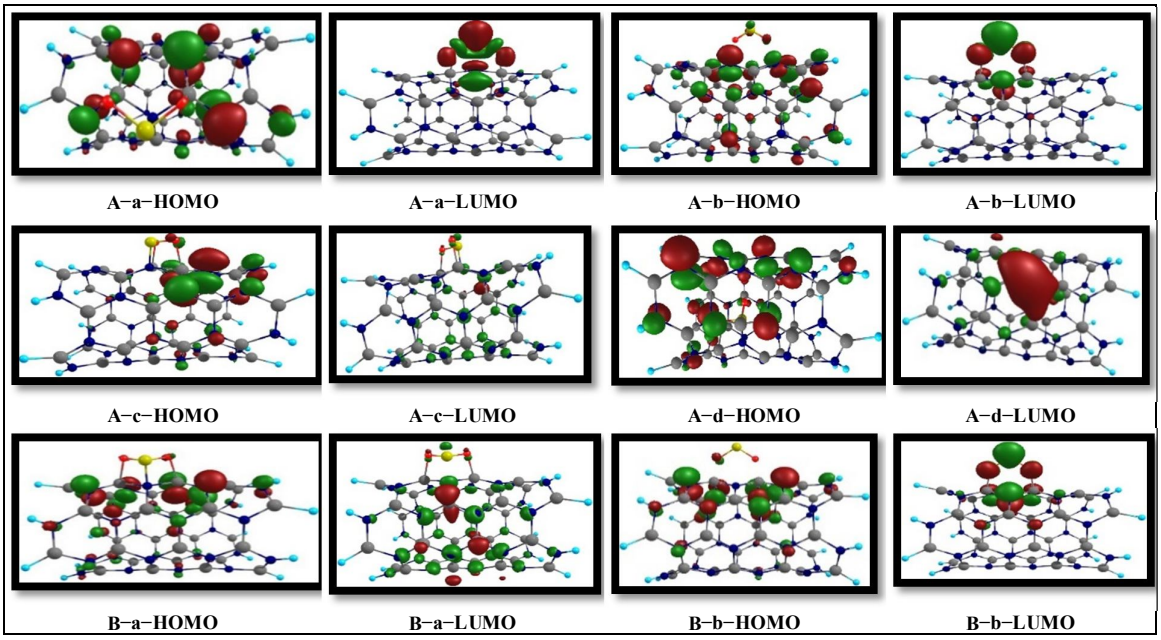

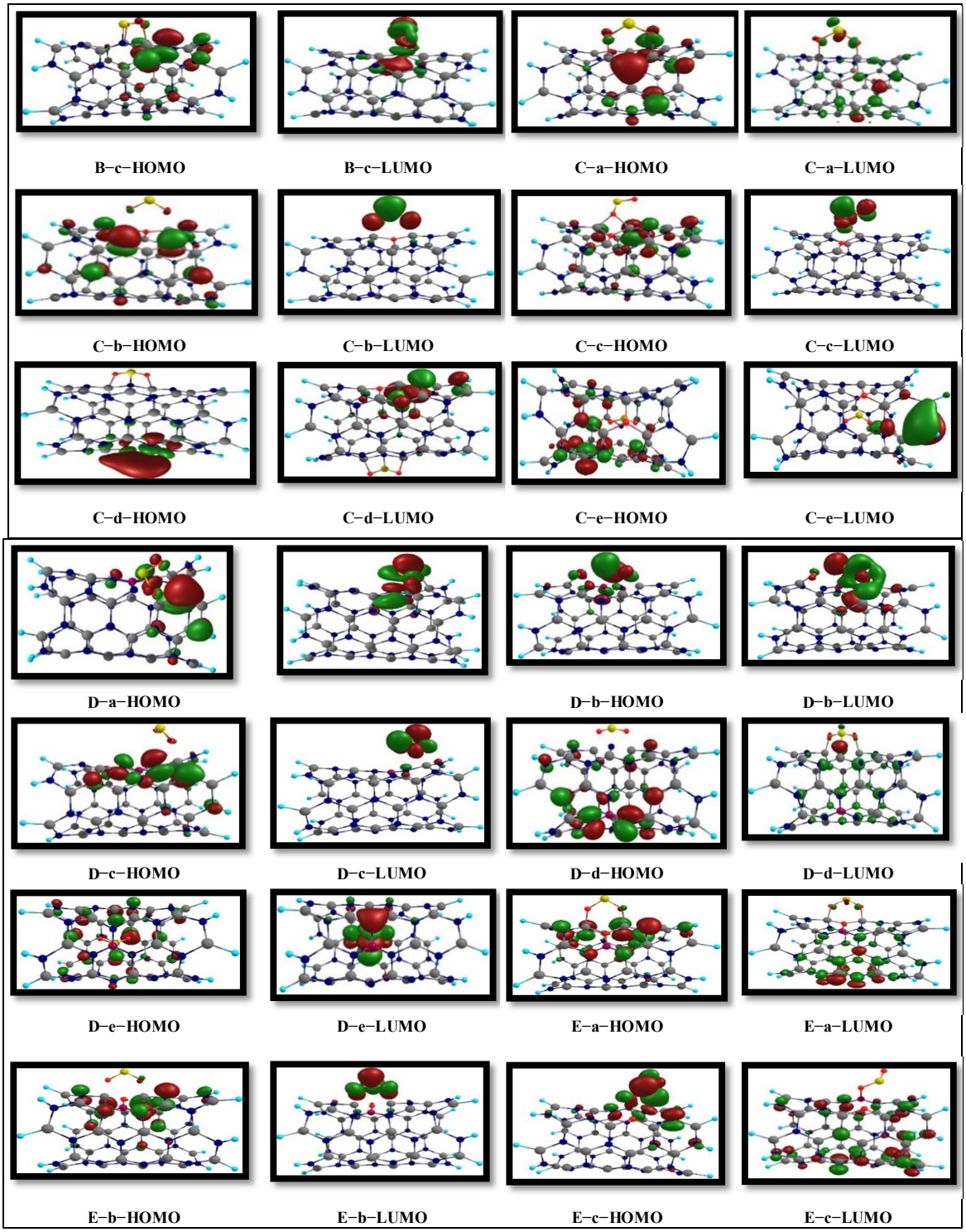
B–c–HOMO
B–c–LUMO
C–a–HOMO
C–a–LUMO
C–b–HOMO
C–b–LUMO
C–c–HOMO
C–c–LUMO
C–d–HOMO
C–d–LUMO
C–e–HOMO
C–e–LUMO
D–a–HOMO
D–b–HOMO
D–b–LUMO
D–c–HOMO
D–c–LUMO
D–d–HOMO
D–d–LUMO
D–e–HOMO
D–e–LUMO
E–a–HOMO
E–a–LUMO
E–b–HOMO
E–b–LUMO
E–c–HOMO
E–c–LUMO

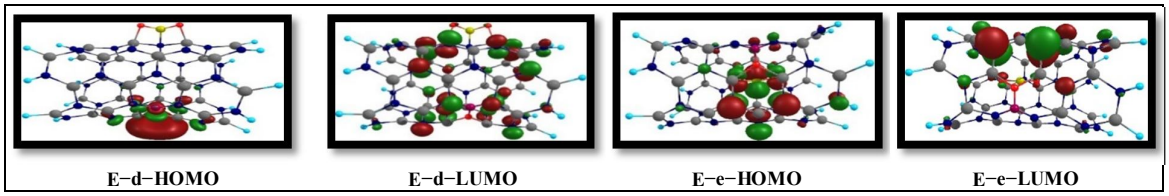

Fig. 2. Plots of HOMO and LUMO energy structures for adsorption SO_2 gas on the surface of pristine and B, O and B&O doped of (4, 4) armchair model of AlNNTs for (A−a to E−e models see Fig 1).

As it can see the LUMO orbital densities for A−a, A−b, B−b, B−c, C−a, C−b, C−c, D−a, D−b, D−c, and F−b models are localized around SO_2 molecule and this result confirm that the SO_2 molecule has a donor electron effect on the nanotube surface. On the other hand, at the A−c, B−a, C−d, C−e, D−d, E−a, E−c and E−d models the LUMO orbitals are dispersed around nanotube surface. The HOMO and LUMO energies of all adsorption models are in range −6.54 to −3.76eV and −5.20 to −1.72eV. It is notable that the HOMO energy of C−d1 model and LUMO energy of E−e1 model is lower than other those models. After adsorbing SO_2 gas and B, O and B&O doped the conduction levels slightly moves to alter energies and it leads to changes in the energy gap. The HOMO−LUMO energy gap (E_{gap}) is one of the key parameters with which to distinguish the electronic stability of the resulting interactions. The calculated E_{gap} value for all adsorption models is in range 0.88 to 4.55 eV. In order to gain a deeper insight over the adsorption process, the electronic properties of all adsorption models are investigated by density of states (DOS) plots. The DOS plots of unabsorbed models and the absorbed nanotube are shown in the Figs 3. Comparison of DOS plots of the pristine and B, O and B&O doped AlNNTs demonstrate that the electronic properties of nanotube after doping B and O atoms are significantly altered specially in α−spin model. It indicates a decrement in the E_{gap} of nanotube from 4.44 eV in pristine model to 1.78 and 2.5 eV in α−spin of O and B&O doped a change of −59.99 % and −43.69 %, respectively. While the E_{gap} of nanotube in B doped and β−spin of O and B&O doped decrease slightly from original values. It is notable that the E_{gap} of nanotube decrease from 4.44 eV in pristine model to 0.88 eV in the B−b adsorption models a change of −80.18% and the conductivity of nanotube increase significantly from original values; these properties are favorable to making the SO_2 detector or sensor. Therefore, we find that the E−e−β model has the lowest conductivity whereas the B−b model has the highest conductivity among all studied species.

For study the electrical properties of SO_2/nano complex, the changes of the Fermi level energy (E_{FL}) of system are calculated and results are given in Tables 1−3. Comparison results indicate that the E_{FL} of adsorbent after the interaction with SO_2 reduce from −4.20 eV in pristine state to −4.39, −4.62, −5.64 eV in the A−a, A−B, B−b models respectively.

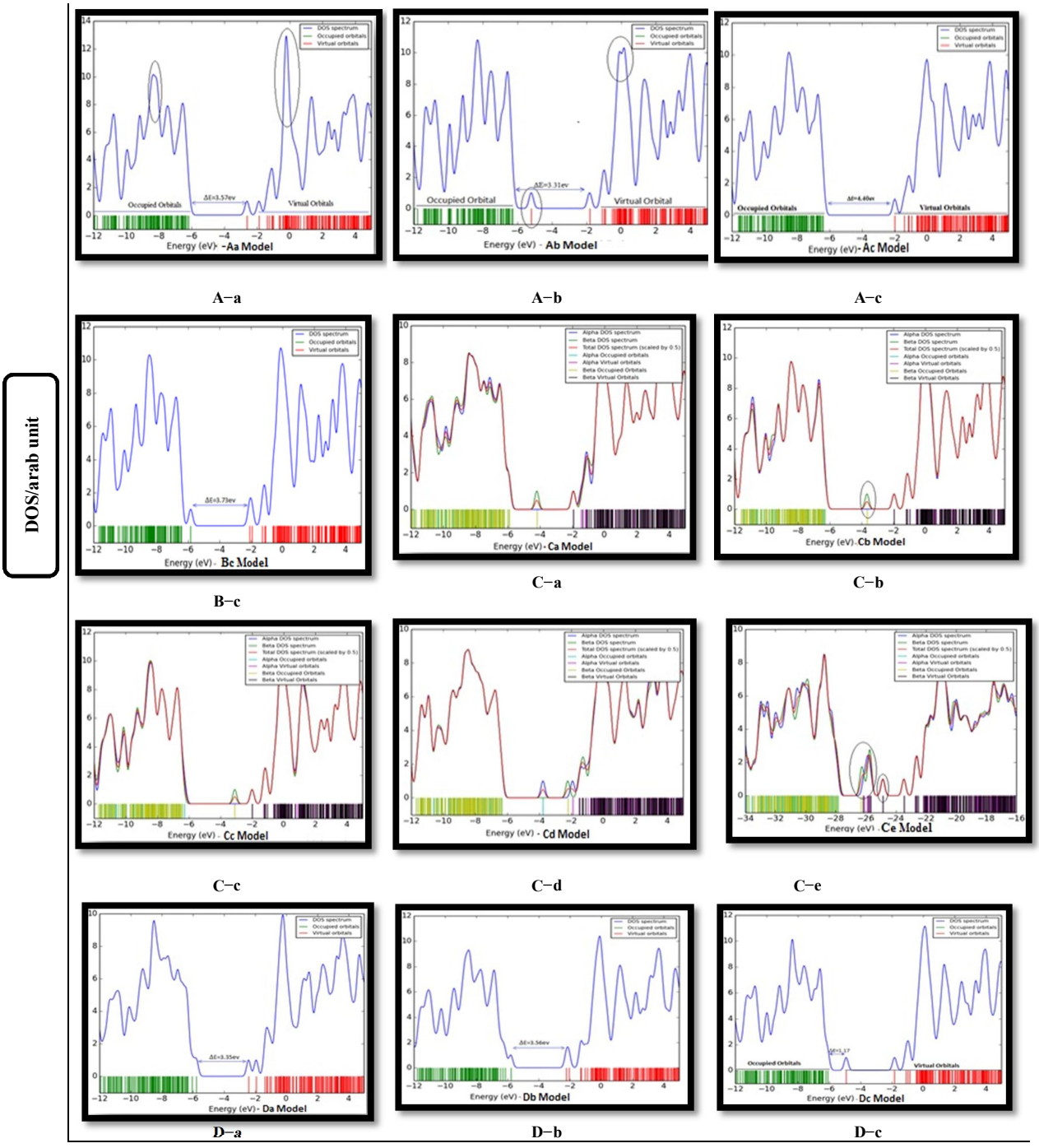
DOS/arab unit
Energy (eV)- Aa Model
Occupied Orbitals
Virtual Orbitals
ΔE=3.57ev
A−a
Energy (eV) - Ab Model
Occupied Orbital
Virtual Orbital
ΔE=3.31ev
A−b
Energy (eV)- Ac Model
Occupied Orbitals
Virtual Orbitals
Δ=4.40ev
A−c
Energy (eV) - Bc Model
ΔE=3.73ev
B−c
Energy (eV) - Ca Model
C−a
Energy (eV) - Cb Model
C−b
Energy (eV) - Cc Model
C−c
Energy (eV) - Cd Model
C−d
Energy (eV) - Ce Model
C−e
Energy (eV) - Da Model
ΔE=3.35ev
D−a
Energy (eV) - Db Model
ΔE=3.56ev
D−b
Energy (eV) - Dc Model
Occupied Orbitals
Virtual Orbitals
D−c

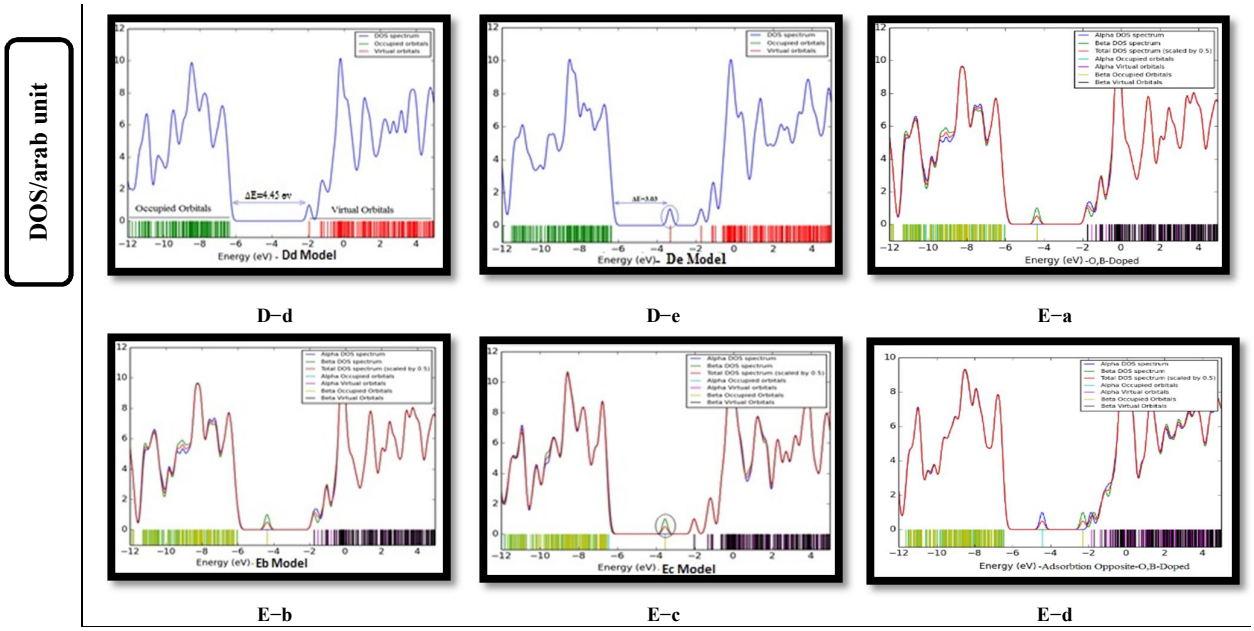

Fig. 3. DOS Plots for adsorption SO_2 gas on the surface of pristine and B, O and B&O doped of (4, 4) armchair model of AlNNTs for (A−a to E−e models see Fig 1).

The E_{FL} of the C−a, C−b and C−c models (α−spin of the O−doped AlNNTs) decreases significantly to −5.03, −4.97 and −4.73 respectively. And also the E_{FL} of the D−c and D−e (B−doped) models decrease significantly from −4.10 eV to −5.49 and −4.83eV respectively. Moreover the E_{FL} of α−spin in the E−a, E−b and E−c models (B&O−doped) decreases significantly from −2.99 eV to −5.18, −5.18 and −5.03eV respectively. On other hand, the E_{FL} of other models increase significantly from original values. The changes of Fermi level energies demonstrate a remarkable number of electrons transfer during the interaction between adsorbate and adsorbent that cause the redistribution of system charges and lead to the changes in the electronic structure of the adsorption system, which significantly affected the electrical conductance of system.

By using Fermi level energy, the work function parameters (Δϕ) of systems are calculated using follow equation:

$$\Delta\phi = E_{\inf} - E_{FL} \qquad (11)$$

here E_{inf} is the electrostatic potential at infinity and E_{FL} is the Fermi level energy. In this consideration, the electrostatic potential at infinity is assumed to be zero.

The work function parameter of a system is the least amount of energy required to remove an electron from the Fermi level to a point far enough not to feel any influence from the material [64]. The emitted electron current densities in a vacuum are theoretically described by the following classical equation:

$$j = AT^2 \exp^{(-\Delta\phi/kT)} \qquad (12)$$

where A is called the Richardson constant (A/m2), T is the temperature (K). Inspection of results in Tables 1−3 indicate that the work function for the pristine, O, B and B&O−doped AlNNTs is 4.20, (2.8 eV for α spin and 4.22eV for β spin), 4.10 eV and (2.99 eV for α spin and 4.16 eV for β spin) respectively. The emitted electron current density is exponentially related to the negative value of $\Delta\phi$. Comparison results display that the work function of α

spin of O and B&O‑doped AlNNTs decrease significantly from pristine model and so the emitted electron current densities of nanotube increase significantly from original state.

As displayed in Tables1‑3, it is found that the adsorption of SO_2 gas at all models except of B−c, A−C and D−b models the work functions of nanotube increase significantly from unabsorbed models. These results demonstrate that the O, B, B&O doping process provides a good strategy for improving the sensitivity of AlNNTs to toxic SO_2 gas.

It is known that, the global hardness of compound is specified as its endurance toward deformation in the presence of an electric field. Increasing in global hardness leads to increase in stability and diminish in reactivity of the species [65].

With doping O and B&O atoms the global hardness of the α spin nanotube decrease significantly from original values, whereas the global hardness of B‑doped , β spin of O and B&O‑doped nanotube slightly alter. As it can see in Tables 1‑3, the global hardness of the A−a, A−b, B−b, B−c, D−a, D−b, D−b and D−c models decrease significantly from original values and at the other models this parameter changes slightly from original values.

The values of electronic chemical potentials (μ) for all adsorption models except B−c, C−a−β and E−d−α model decrease significantly from original state. However, the electrophilicity parameters of nanotube at all adsorption models except of B−b, C−a−β, C−b−β, C−c−β, E−a−β, E−c and E−e−β increase from unabsorbed models.

The charge transfer parameters (ΔN) of all adsorption models are positive. The positive values of ΔN and reduction of the global hardness and electronic chemical potentials of nanotube/SO_2 complex indicate that when SO_2 gas is chemisorbed on the surface of the pristine, O, B, B&O‑doped AlNNTs, a fairly large charge transfer to the SO_2 could occur, which suggests that their electronic transport properties could be notably changed upon chemisorption's of SO_2. The direction of electron flow will be characterized via electronegativity or chemical potential. When SO_2 gas is added to the pristine and O, B&O− nanotube electrons transfer from the higher chemical potential to the lower chemical potential, until the electronic chemical potentials become identical. As a result, electrons will flow from a definite occupied orbital in a nanotube and will go into a definite empty orbital in a SO_2. The global electrophilicity index determines the energy lowering of a ligand due to maximum flow of electron from donor to acceptor species and provides information about structural stability, reactivity and toxicity of chemical species.

Molecular electrostatic potential

To further investigate the electrical properties and charge distribution around adsorption position of nanotube/SO_2 system we calculate the molecular electrostatic potential (ESP) plots. In the ESP plots, the blue color represents the positive charges or the electrophilic regions and the red color represents the negative charges or the nucleophilic regions, the MEP plots are depended to nanotube radius [66‑68]. The calculated ESP and contour plots of all adsorption models are shown in Fig. 4.

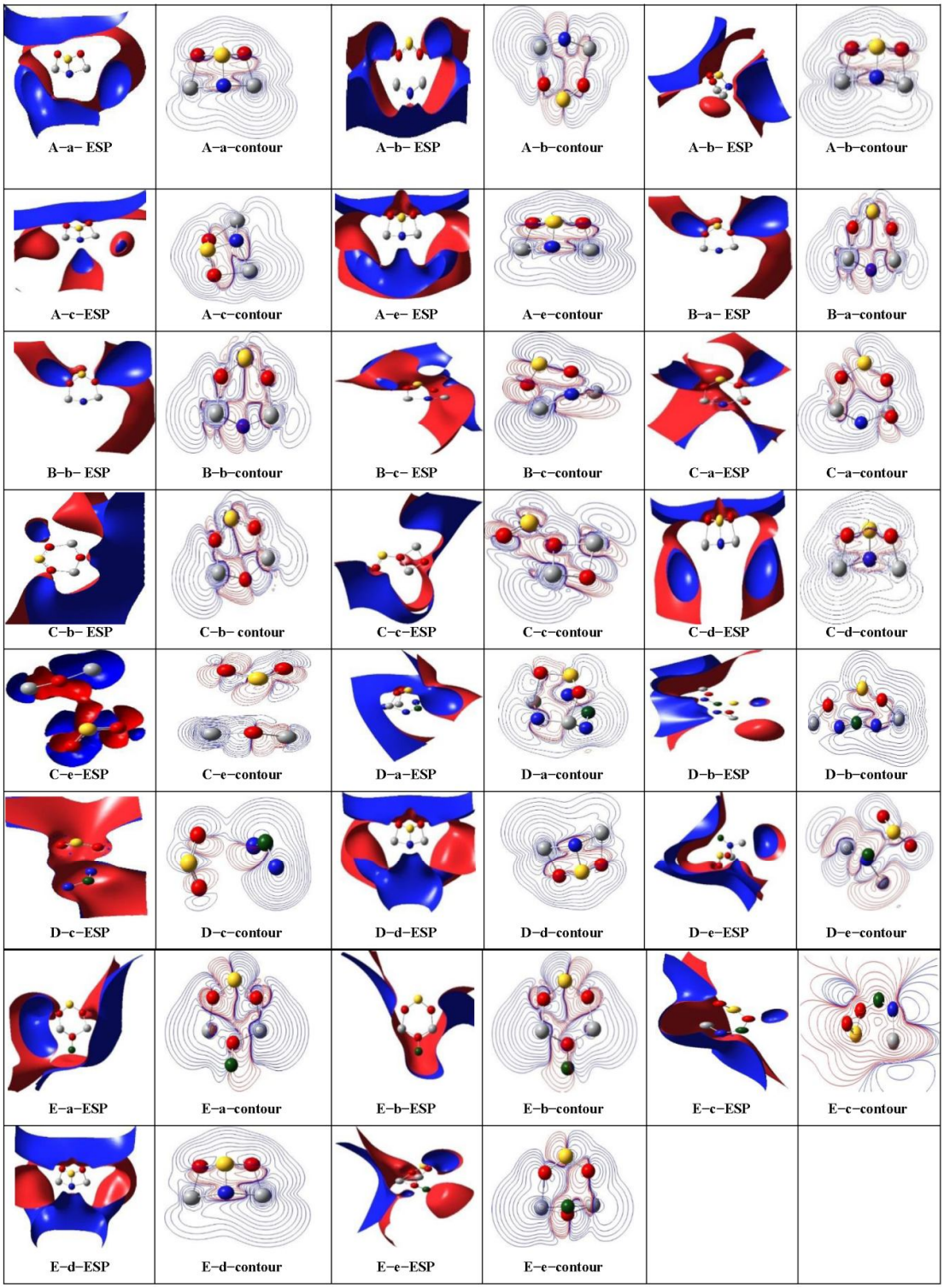

Fig. 4. The ESP and contour Plots for adsorption SO_2 gas on the surface of pristine and B, O and B&O doped of (4, 4) armchair model of AlNNTs for (A−a to E−e models see Fig 1).

The ESP plots indicate that the most electron density and negative potential, red color is localized around adsorption position and above adsorbate. The most positive electrostatic potential (blue color) occurs over nanotube surface. The distribution of electrostatic potential is depended on orientation of SO_2 adsorption and doping atoms. Comparison results reveal that in the A−a, A−b, A−e, C−b, C−d, C−e, D−d, E−a, E−c and E−d models a maximum density of electrostatic potential is distributed around adsorption position, and the ESP density around adsorption position is more than other adsorption model.

The ESP plots results demonstrate that a low charge transfer is occurred from the SO_2 gas toward nanotube resulting in a weak ionic bonding in the AlNNTs surface. Therefore, it is expected that the interaction of SO_2/nanotube complex, after adsorption process, caused that the exterior layer of nanotube rich of charge. On the other hand contour plot results indicate that the positive regions of electrostatic potential are localized above and below the central atom in SO_2 for which the sulfur in SO_2 is more positive than the central oxygen. However, the negative electrostatic potentials and the positive potentials are localized over the nitrogen and aluminum atoms respectively.

Natural bonding orbital analysis

The natural bond orbital (NBO) analyses are applied to reach more details about interaction between adsorbent and adsorbate [69]. For this aim the NBO analysis and stabilization energy $E^{(2)}$ for all adsorption models are calculated from second order perturbation theory analysis of the Fock−matrix . The stabilization energy $E^{(2)}$ calculated by follow Eq:

$$E^{(2)} = q_i \frac{F_{ij}^2}{\varepsilon_j - \varepsilon_i} \qquad (13)$$

where F_{ij} is the off−diagonal NBO Fock−matrix element, ε_i and ε_j are orbital energies and q_i is donor orbital occupancy. The electron donor orbital *i*, electron acceptor orbital *j*, and stabilization energy $E^{(2)}$ between their interaction for the selected donor − acceptor bonds are shown in Fig. 5.

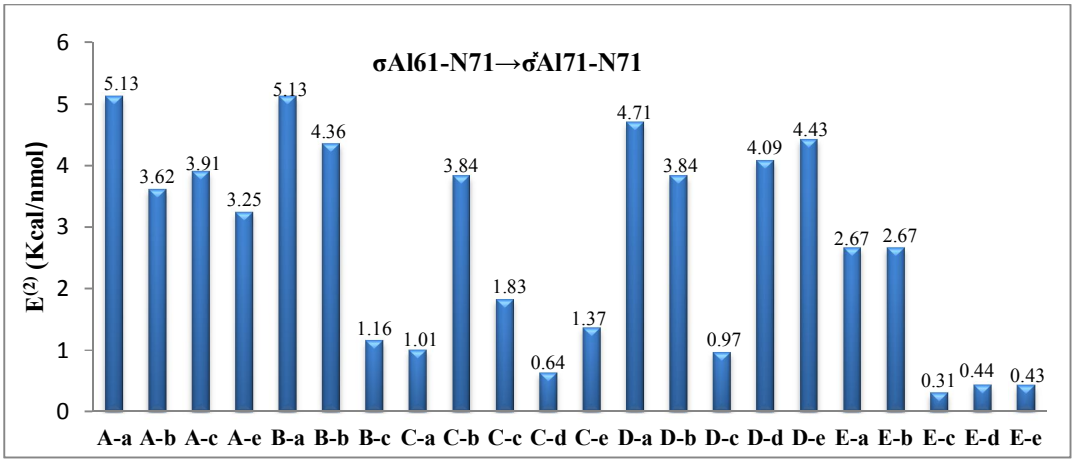

Fig. 5. The stabilization energy $E^{(2)}$ Plots for adsorption SO_2 gas on the surface of pristine and B, O and B&O doped of (4, 4) armchair model of AlNNTs for (A−a to E−e models see Fig 1).

As displays in Fig. 5, the intermolecular interaction is formed by the orbital overlap between bond orbital σAl61−N71→σ*Al71−N71 at the A, B, C, D and E models have more stabilization energy between other those interaction. Comparison results indicate that stabilization energy $E^{(2)}$ of the A−a and B−a models is more than other adsorption models. The results reveal that doping O, B, and B&O atoms reduce the stabilization energy. Moreover, the stabilization energy of system is depended on the orientation of SO_2 adsorption. The stabilization energy of system at the (a) orientation of all adsorption models are in order: A−a = B−a > D−a> E−a > C−a. It is notable that doping O atom decreases the stabilization energy of system of C−a model significantly than other models.

Comparison results reveal that doping O atom in all adsorption models decrease the $E^{(2)}$ and so weaker charge transfer interaction occurred in them. These facts may be the probable reasons behind the relative stability of the axial and equatorial adsorption SO_2 gas on the outer and inner surface of nanotube based on energetic data and NBO interpretation. Furthermore, the NBO analysis specifies hybridization of Al and N atoms of nanotube and S atom of SO_2 gas is sp^2 during the adsorption process. We found that when O atoms dopants, the charge transfer between donor and acceptor orbital decrease significantly from original values, on the other hand the orientation of SO_2 adsorbent alter significantly the charge transfer.

NMR parameters

Nuclear magnetic resonance (NMR) is one of the important techniques to investigate the structural parameters of material. NMR measures the local magnetic fields on nuclei, generated by response of electrons to an external uniform magnetic field. NMR techniques are applied to produce high external magnetic fields and some kind of internal interaction; i.e. the spin–spin interaction in NMR [70−71]. To study the effects of B, O, B&O doped and SO_2 adsorption on the structural of the properties of AlNNTs the NMR parameters including CSI and CSA chemical shielding and NMR spectrum of all adsorption models are calculated and results are given in Fig 6.

The adsorption of SO_2 gas and doping of B,O and B&O atoms in N51 and Al51 site of AlNNTs changes the electrostatic environment of the around position which are directly chemically bond to dopant atoms and adsorbent. The obtained results show that the isotropy and asymmetry parameters of the Al32, Al62, N33 and N33 sites are more than other sites. Furthermore, the isotropy the electrostatic properties of nuclei are mainly dependent on electronic density at their sites, therefore because of the SO_2 gas adsorption, the electronic densities of nuclei and the CS tensors undergo changes. Moreover, the CSI values of the Al and N atoms alter by adsorbing SO_2 gas on doped nanotube, indicating less electronic around the Al and N nucleus. The obtained results confirm that the B, O and B&O atom contribute to weaker chemical bonding with adsorbing atom. This result confirms that the strongest intermolecular interaction will result in a slightly alter in diamagnetic shielding.

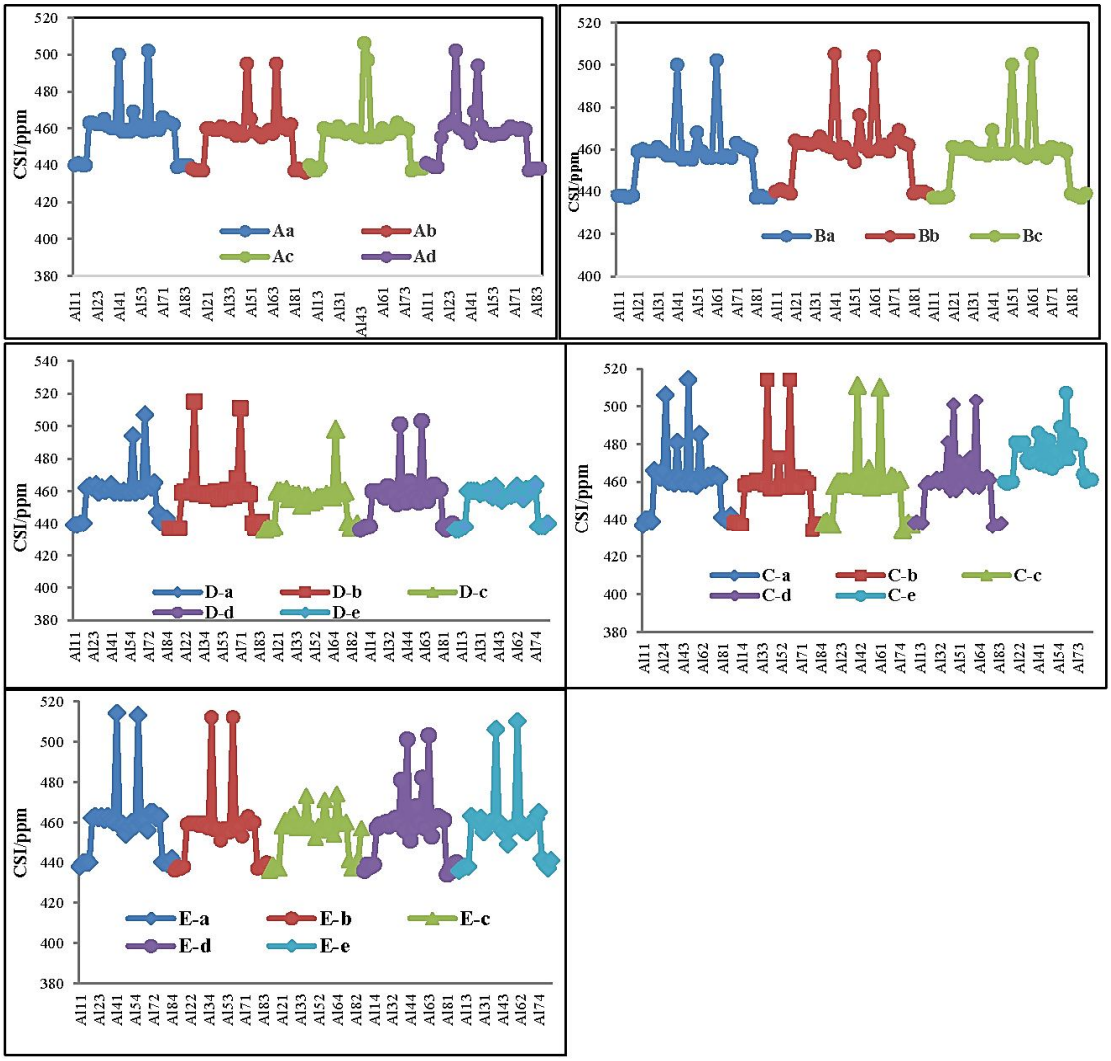

Fig. 6. The CSI parameters of Al nuclei for adsorption SO_2 gas on the surface of pristine and B, O and B&O doped of (4, 4) armchair model of AlNNTs for (A−a to E−e models see Fig 1).

CONCLUSIONS

In this research, the electrical and structural properties of the SO_2 gas adsorption on the surface of the pristine, B, O and B&O doped (4, 4) armchair AlNNTs by using DFT method at cam−B3LYP/6−31G (d) level of theory. Inspections of results demonstrate that the adsorption energy of all adsorption models is negative and all adsorption models are exothermic and favorable in thermodynamic approach. Doping of B atom at the C models increase the adsorption energy significantly from original values, whereas doping O atom in D models decrease the adsorption energy significantly from original values. The calculated E_{gap} value for all adsorption models is in range 0.88 to 4.55 eV. The positive values of ΔN and reduction of the global hardness nano/SO_2 complex indicate that the nanotube has a donor electron effect. In the A−a, A−b, A−e,

C−b, C−d, C−e, D−d, E−a, E−c and E−d models, a maximum density of electrostatic potential is distributed around adsorption position, and the ESP density around adsorption position is more than other adsorption model.

REFERENCES

[1] S. Iijima, Nature 354 (1991) 56–58.

[2] P. J. Pauzauskie, P. Yang, Today 6 (2006) 36–38.

[3] T. C. Dinadayalane, A. Kaczmarek, J. Lukaszewicz, J. Leszczynskiled carbon nanotubes. J. Phys. Chem. C 111(2007) 7376–7383.

[4] T. C. Dinadayalene, J. S. Murray, M. C. Concha, P. Politzer, J. Leszczynski, J. Chem. Theory. Com. 6 (2010) 1351–1357.

[5] G. Stan, C. Ciobanu, T. Thayer, G. Wang, J. Creighton, K. Purushotham, L. Bendersky, R. Cook, Nanotechnol. 20 (2009) 35706–357014.

[6] Z. Peralta−Inga, S. Boyd, J. S. Murray, C. J. O'Connor, P. Politzer, Struct. Chem. 14 (2003) 431–443.

[7] Y. Taniyasu, M. Kasu, T. Makimoto, Nature. 441 (2006) 325–328.

[8] P. Ruterana, M. Albrecht, J. Neugebauer, handbook on materials and devices. Wiley, New York. (2003).

[9] T. Oto, R. G. Banal, K. Kataoka, M. Funato, Y. Kawakami, Nat. Photonics. 4 (2010) 767–770.

[10] Y. Taniyasu, M. Kasu, T. Makimoto, Appl. Phys. Lett. 84 (2004) 115-119.

[11] N. Kuramoto, H. Taniguchi, I. Aso, Am. Ceram. Soc Bull. 68 (1989) 883–887.

[12] M. S. Shur, R. Gaska, IEEE. T. Electron. Dev. 57(2010)12

[13] J. Deng, Y. Bilenko, A. Lunev, X. Hu, T. M. Katona, J. Zhang, M. S. Shur, R. Gaska, J. Appl. Phys. 46 (2007) 263.

[14] L. W. Yin, Y. Bando, Y. C. Zhu, M. S. Li, Y. B. Li, D. Golberg D, Adv. Mater. 17 (2005) 110−117.

[15] J. Beheshtian, A. Ahmadi Peyghan, Z. Bagheri, J. Mol. Model. 19 (2013) 2197–2203.

[16] M. Rezaei−Sameti, E. Samadi Jamil E, J. Nanostruct. Chem. 6 (2016) 197–205.

[17] A. Ahmadi, J. Beheshtian, N. L. Hadipour, Physica E. 43 (2011) 1717–1719.

[18] A. Ahmadi Peyghan, A. Omidvar, N. L. Hadipour, Z. Bagheri, M. Kamfiroozi, Physica E. 44 (2012) 1357–1360.

[19] A. Ahmadim, M. Kamfiroozi, J. Beheshtian,N .L. Hadipour, Stru. Chem. 22 (2011) 1261-1270

[20] G. Stan, C. V. Ciobanu, T. P. Thayer, G. T. Wang, J. R. Creighton, K. P. Purushotham, L. A. Bendersky, Nano. Techn. 20 (2008) 3−10.

[21] A. Soltani, M. Ramezani Taghartapeh, H. Mighani, A. Allah Pahlevani, R. Mashkoor, App. Surface. Sci. 259 (2012) 637–642.

[22] J. Beheshtian, Z. Bagheri, M. Kamfiroozi, A. A. Ahmadi, Structural. Chem. 23 (2012) 653–657.

[23] J. Beheshtian, M. T. Baei, Z. Bagheri, A. Ahmadi Peyghan, Micro. Electro. J. 43(2012) 452–455.

[24] M. Noei, M. Ebrahimikia, Y. Saghapour, M. Khodaverdi, A. A. Salari, N. Ahmadaghaei, J. Nanostruct. Chem. 5 (2015) 213–217.

[25] M. T. Baei, A. Ahmadi Peyghan, Z. Bagheri, Chin. Chem. Lett. 23 (2012) 965–968.

[26] M. Rezaei−Sameti, Physica E. 43 (2011) 1249–1254.

[27] A. Ahmadi, N. L. Hadipour, M. Kamfiroozi, Z. Bagheri, Sensors Actuators. B. Chem. 161 (2012)1025–1029.

[28] S. H. Lim, J. Lin, Chem. Phys. Lett. 466 (2008) 197–204.
[29] J. Beheshtian, A. Ahmadi Peyghan, Z. Bagheri, J. Mol. Model. 19 (2013) 2197–2203.
[30] H. R. Masoodi, A. Ebrahimi, S. Bagheri, Structural Chem. 26 (2015) 1013–1024.
[31] M. T. Baei, S. Hashemian, P. Torabi, F. Hosseini F, Fullerenes, Nanotubes and Carbon Nanostr. 23 (2015) 263−265.
[32] Z. Mahdavifar, M. Haghbyan, M. Abbasi. Sensors and Actua. B. Chem. 196 (2014) 555–566.
[33] J. Beheshtian, M. T. Baei, A. Ahmadi Peyghan, Z. Bagheri, J. Mol. Model. 19 (2013) 943–949.
[34] M. Najafi, App. Surf. Sci. 384 (2016) 380–385.
[35] M. Noei, M. Ebrahimikia, N. Molaei, M. Ahadi, A. A. Salan, O. Moradi, Russian. J. Phys. Chem. A. 90 (2016) 2221–2229.
[36] A. Ahmadi Peyghan, M. T. Baei, S. Hashemian, P. Torabi, J. Mol. Model. 19 (2013) 859–870.
[37] M. D. Esrafili, Canadian. J. Chem. 19 (2013) 711−717.
[38] Z. Mahdavifar, M. Haghbayan, App. Sur. sci. 263 (2012) 553–562.
[39] M. Noei, A. A. Salari, N. Ahmadaghaei, Z. Bagheri, A. Ahmadi Peyghan, Comp. Rend. Chim. 16 (2013) 985–989
[40] M. Samadizadeh, S. F. Rastegar, A. Ahmadi Peyghan, Physica E. 69 (2015) 75–80.
[41] A. Seif, L. Torkashavand, F. Mohammadi, Open Chem. 12 (2013) 131–139.
[42] A. Soltani, A. Sousaraei, M. Mirarab, H. Balakheyli, J. Saudi. Chem. Soc. 21 (2017) 270−276.
[43] A. Soltani, M. Ramezani Taghartapeh, E. T. Lemeski, M. Abroudi, H. Mighani, Superlat. Micro struc. 58 (2013) 178–190.
[44] M. T. Baei, A. Ahmadi Peyghan, Z. Bagheri, Physica E. 47 (2013) 147–151.
[45] J. Beheshtian, A. Ahmadi Peyghan, Z. Bagheri, Physica E. 44 (2012)1963–1968.
[46] A. Ahmadi Peyghan, M. T. Baei, P. Torabi, S. Hashemian, J. Phosphorus, Sulfur, and Silicon nd the Related Elements. 188 (2013) 1172−1177.
[47] Z. Mahdavifar, N. Abbasi, E. Shakerzadeh, Sensors Actuat. B. Chem. 185 (2013) 512–522.
[48] Z. Mahdavifar, N. Abbasi, Physica. 56 (2014) 268–276.
[49] Z. Mahdavifar, N. Abbasi, E. Shakerzadeh, J. Mol. Liquids. 204 (2015) 147–155.
[50] M. T. Baei, M. Ramezani Taghartapeh, E. T. Lemeski, A. Soltani, Superlat Micro struc. 72 (2014) 370–382.
[51] S. Kamalinahad, M. Solimannejad, E. Shakerzadeh, Superlat Micro struct. 289 (2016) 390–397.
[52] H. C. Michael, National Council for Science and the Environment. Washington DC. (2010)
[53] G. A. Atlanta, Toxicological Profile for Sulfur Dioxide. Atlanta, GA: U.S. Department of Health and Human Services, Public Health Service (1998)
[54] C. C. Cid, G. Jimenez−Cadena, J. Riu, A. Maroto, F. Xavier Rius, G. D. Batema, G. vanKoten, Sens. Actuators B. Chem. 141 (2009) 97–103.
[55] X. Zhou, Q. J. Pan, M. X. Li, B. H. Xia, H. X. Zhang, J. Mol. Struct: THEOCHEM. 822 (2007) 65–73.
[56] Z. Y. Denga, J. M. Zhanga, K. W. Xub, Appl. Surface Sci. 347 (2015) 485–490.

[57] J. Beheshtian, M. T. Baei, A. Ahmadi Peyghan, Z. Bagheri, J. Mol. Model. 18 (2012) 4745–4750
[58] S. F. Rastegar, N. L. Hadipour, H. Soleymanabadi, J. Mol. Model. 20 (2014) 2439−2442.
[59] M. L. Zhang, T. Ning, S. Y. Zhang, Z. M. Li, Z. H. Yuan, Q. X. Cao, Mat. Sci. Semicond. Process. 17 (2014) 149–154.
[60] [60] R. Ditchfield, W. J. Hehre, J. A. Pople, J. Chem. Phys. 54 (1972)724.
[61] M. W. Schmidt, K. K. Baldridge, J. A. Boatz, S. T. Elbert, M. S. Gordon, et al. J. Comp. Chem. 14 (1993) 1347−1363
[62] M. Rezaei−Sameti, S. Yaghoobi, Comp. Condense Mat. 3(2015) 21−29.
[63] M. Rezaei Sameti, Physica B. 407 (2012) 22–26.
[64] S. Stegmeier, M. Fleischer, P. Hauptmann, Sens. Actu. B. Chem. 148 (2010) 439−449.
[65] A. Ahmadi Peyghan, A. Soltani, A. Allah Pahlevani, Y. Kanani, S. Khajeh, App. Surface Sci. 270 (2013) 25– 32.
[66] Z. Peralta−Inga, P. Lane, J. S. Murray, S. Boyd, M. E. Grice, C. J. O'Connor, P. Politzer, Nano. Lett. 3 (2003) 21–28.
[67] F. A. Bulat, A. Toro−Labbé, T. Brinck, J. S. Murray, P. Politzer, J. Mol. Model. 16 (2010) 1679–1691
[68] F. A. Bulat, J. S. Burgess, B. R. Matis, J.W. Baldwin, L. Macaveiu, J. S. Murray, P. Politzer, J. Phys. Chem. A. 116 (2012) 8644–8652.
[69] E. Glendening, A. Reed, J. Carpenter, F. Weinhold, NBO, Version 3.1, GaussianInc., Pittsburg, PA, CT. (2003).
[70] D. Canet, Nuclear Magnetic Resonance: Concepts and Methods.Wiley, Chichester (1996)
[71] D. G. Gory, A. F. Fahmy, T. F. Havel, Natl. Acad. Sci U.S.A. 94 (1997) 1634–1639.